Synthesis and photophysical characterization of phosphorescent platinum(II) bis-(trimethylsilyl)ethynyl-phenanthroline organometallic complexes with bis-arylethynyl derivatives

Michito Shiotsuka * **· Taiki Asano · Yoshihiro Kurono · Rikuo Ono · Ryuta Kawabe**

Graduate School of Engineering, Nagoya Institute of Technology,

Gokiso, Showa, Nagoya, Aichi 466-8555, Japan

* Corresponding author

E-mail address: michito@nitech.ac.jp (M. Shiotsuka).

Received:

Abstract

Phosphorescent platinum(II) phenanthroline organometallics, Pt(3,8-Phen≡TMS)(≡Ph-R)$_2$, of respective arylethynyl ligands with different substituents (R = H (**1**), 4-Me (**2**), 4-*t*-Bu (**3**), 4-F (**4**), 3-F (**5**), 2-F (**6**), 3,5-di-*t*-Bu (**7**), 4-CF_3 (**8**), 3,5-di-CF_3 (**9**), 4-COOMe (**10**), 4-NO_2 (**11**)) were synthesized by transmetalation with copper(I) ion. The visible luminescence of these organometallics in deoxygenated CH_2Cl_2 was assigned to the phosphorescence, and the DFT calculations of 11 organometallics clearly supported the assignment of phosphorescence from the mixed transition of ^{3}MLCT/^{3}LLCT (LLCT = ligand-to-ligand charge transfer). A good linear correlation between the observed emission energy values of phosphorescence and the calculation values of the difference between the lowest excited triplet state and the ground singlet state by DFT or TD-DFT was obtained, and this correlation reflected that the related MOs of these complexes are included in both MLCT and LLCT under the photo-excited triplet state.

Keywords: Platinum: Phenanthroline: Phosphorescence: DFT calculation

1. Introduction

Research regarding many kinds of phosphorescent metal complexes continues to inspire highly efficient phosphorescence with respect to their potential applications in the fields of photovoltaics and organic light-emitting diodes as well as to biological applications [1-5]. Particularly, phosphorescent studies of platinum(II) and ruthenium(II) complexes have been reported by many groups compared to those of other metal complexes because of the efficient emissions and long emission lifetimes of platinum(II) and ruthenium(II) complexes [6-9].

Photophysical studies of ruthenium(II) polypyridine complexes have found that the phosphorescence was attributable to the ^{3}MLCT transition from the photo-excited state. The ^{3}MLCT emission energy was usually tuned to prepare many kinds of polypyridine ligands as bipyridine derivatives with different substituents because the lowest unoccupied molecular orbital (LUMO) in their complexes was mainly assignable to π* orbitals on the polypyridine [9]. However, the highest occupied molecular orbital (HOMO) was mainly d orbitals on ruthenium ion, and the tuning of phosphorescent energy was less effective.

On the other hand, platinum(II) organometallic complexes with bipyridine derivatives and two various arylethynyl ligands, Pt(L)(≡-aryl)$_2$ (L = bipyridine derivatives), have recently focused attention on unique emissive properties such as vapochromism, mechanochromism, and solid emission [10-19]. Photophysical studies of these complexes indicated that the emission of these complexes in solution was attributable to the mixed transition of ^{3}MLCT and ^{3}LLCT (LLCT = ligand-to-ligand charge transfer) from the photo-excited state [20-23]. Then, the phosphorescent energy of these platinum complexes could be tuned by using various arylethynyl ligands with different substituents because HOMO in their complexes includes π orbitals on respective arylethynyl ligands. We therefore became interested in the phosphorescent energy tuning of platinum(II) organometallic complexes with many arylethynyl ligands, Pt(L)(≡-aryl)$_2$, and the estimation of the effect among different arylethynyl ligands for phosphorescent energy by using DFT and TD-DFT calculation.

We report herein the synthesis and photophysical characterization of novel platinum(II) organometallic complexes with phenanthroline derivatives and 11 respective arylethynyl ligands with different substituents (**Pt(3,8-Phen≡TMS)(≡Ph-R)$_2$**: **R** = H (**1**), 4-Me (**2**), 4-*t*-Bu (**3**), 4-F (**4**), 3-F (**5**), 2-F (**6**), 3,5-di-*t*-Bu (**7**), 4-CF_3 (**8**), 3,5-di-CF_3 (**9**), 4-COOMe (**10**), 4-NO_2 (**11**)) as shown in Scheme 1. The ligand 3,8-Phen≡TMS is suitable for estimating the effects of different arylethynyl ligands on these platinum complexes because the phenanthroline skeleton is a rigid and planar structure compared to bipyridine or terpyridine and previous platinum organometallics with similar bipyridine ligands have exhibited phosphorescence in solution and unique vapochromism in the solid state [11-16]. These 11 substituents were selected not only the electron donating groups as alkyl substituents and withdrawing groups as nitro substituents but the fluoride substituents for the substitution position effect and bulky substituents as trifluoromethyl substituents for the steric hindrance effect in solid as shown in Scheme 1. Furthermore, we show a

good linear correlation between phosphorescent energy measured by luminescence spectroscopy and the T_1-S_0 energy separation obtained by DFT or TD-DFT calculation.

2. Experimental Section

2.1. Material and measurements

All chemicals used for syntheses were purchased from Aldrich or TCI and used without further purification. All reactions were carried out under an argon atmosphere. Solvents were freshly distilled according to standard procedures. The 3,8-bis-(trimethylsilyl)ethynyl-1,10-phenanthroline (3,8-Phen≡TMS) was synthesized by the similar method of Ziessel et al. [24]. The characterization of the novel platinum complexes has been done by IR, ^{1}H NMR, UV-Vis spectroscopy, and elemental analyses. Elemental analyses for platinum complexes were performed for C, H, and N elements on a Elementar vario EL cube. IR spectra were obtained on a JASCO FT/IR 460 spectrometer using the KBr-pellet method. The ^{1}H NMR spectra were recorded with a Bruker AVANCE and Ascend^{TM} NMR spectrometer (400MHz) at room temperature and the chemical shifts were referenced to CD_2Cl_2 (5.320 ppm). UV-Vis spectra were recorded on a SHIMADZU UV-1800 spectrophotometer in CH_2Cl_2 (emission spectroscopic grade) at room temperature. The corrected emission spectra were measured with a HAMAMATSU C7473 photonic multi-channel analyzer and excitation spectra were recorded on a HITACHI F-2500 fluorescence spectrophotometer. Emission spectra for quantum yield measurement at room temperature were measured in a degassed CH_2Cl_2 (Emission spectral grade) by argon bubbling (over 20min) upon excitation at 425 nm. Emission spectra at 77 K were measured using a liquid nitrogen in a quarts Dewar vessel upon excitation at 425 nm and sample solutions (distilled 2-methyl-THF) in a 5 mm quarts sealed tube were deaerated by freeze-pump-thaw (4 times).

2.2. DFT Calculation Method

DFT and TD-DFT calculations were carried out using the program package *Gaussian 09 Revision C01* [25] at the B3LYP level. At first, the structures of all platinum(II) organometallics under the singlet ground (S_0) state were fully optimized at the restricted B3LYP for the distributions on the molecular orbitals (MOs) in a vacuum state and recalculated in CH_2Cl_2 solution with a polarizable continuum model (PCM) method. The structures of the triplet (T_1) state were fully optimized at the unrestricted B3LYP with same PCM method in CH_2Cl_2 solution. The energy separation, $E(T_1\text{-}S_0)_{DFT}$, between T_1 state and S_0 state was obtained from the energy difference between the highest SOMO under T_1 state and HOMO under S_0 state for comparing phosphorescent energy from the emission spectral data of these complexes. TD-DFT calculation was also performed with restricted B3LYP in CH_2Cl_2 for the comparison between the calculated lowest triplet transition energy, $E(T_1\text{-}S_0)_{TD\text{-}DFT}$, and emission spectral data. The 6-31G(d) basis set was used for C, N, and H atoms, while the effective core potential and the associated valence

basis set was employed with a LanL2DZ basis set for the Pt atom. The spatial plots of MOs were obtained with the program *GaussView 09* [25].

2.3. Preparation of Pt(3,8-Phen≡TMS)Cl_2

Platinum complex Pt(DMSO)Cl_2 (422 mg, 1.0 mmol) was dissolved in dry CH_2Cl_2 (100 ml). The solution was added 3,8-Phen≡TMS (327 mg, 1.0 mmol) and stirred at 30 ˚C for 16 h. The solution was added CH_3CN (20 ml) and CH_2Cl_2 was removed by reduced pressure. The precipitate in CH_3CN was filtered through filter paper and the pale orange powder was obtained. The powder was dried at 60 ˚C under vacuum for 3 h. Yield: 536 mg (84 %).
: FT-IR (KBr, cm^{-1}) ν(Phen-C≡C): 2159, ν(-CH_3): 2852, 2923, 2961. UV/VIS (CH_2Cl_2): λ_{abs} nm (ε × 10^{-5}), 287 (0.46), 328 (0.31), 362 (0.28), 420 (0.03). ^{1}H-NMR (CD_3Cl, 400MHz, ppm): δ = 9.85 (d, J = 1.6 Hz, 2H, Phen-H2 and H9), 8.63 (d, J = 1.6 Hz, 2H, Phen-H4 and H7), 7.95 (s, 2H, Phen-H5 and H6), 0.34 (s, 18H, ≡TMS).

2.4. Preparations of platinum organometallics **1**-**11**

2.4.1. Preparation of Pt(3,8-Phen≡TMS)(≡Ph)$_2$ (**1**)

The Pt(3,8-Phen≡TMS)Cl_2 (255 mg, 0.40 mmol) and ethynylbenzene (100 μl, 0.88 mmol) were dissolved with a mixture solution of dry CH_2Cl_2 (30 ml) and DIPA (3 ml) (DIPA = diisopropylamine) under Ar. The CuI (3.8 mg, 0.02 mmol) was added to the solution. After the mixture was stirred at r.t. for 21 h, MeOH (5ml) was added to the reaction mixture and all solvents were removed by reduced pressure. The crude product was redissolved with CH_2Cl_2 (50 ml) and washed with H_2O (50 ml × 3) by the extraction method. The organic layer was dried over $MgSO_4$ and CH_2Cl_2 was removed by reduced pressure. The residue was purified by SiO_2 chromatography with CH_2Cl_2 as eluent. The yellow powder was washed with Et_2O and dried at 60˚C under vacuum. Yield: 258 mg (84 %).
: Anal. Calcd for $C_{38}H_{34}N_2PtSi_2 \cdot 1/2CH_2Cl_2$: C, 58.6; H, 4.5; N, 3.6. Found: C, 58.8; H, 4.6; N, 3.4. FT-IR (KBr, cm^{-1}) ν(Pt-C≡C): 2116, ν(Phen-C≡C): 2162, ν(-CH_3): 2898, 2958. UV/VIS (CH_2Cl_2): λ_{abs} nm (ε × 10^{-5}), 237 (0.56), 265 (0.78), 281 (0.78), 318 (0.49), 342 (0.45), 359 (0.43), 465 (0.08). ^{1}H-NMR (CD_2Cl_2, 400MHz, ppm): δ = 9.97 (d, J = 1.9 Hz, 2H, Phen-H2 and H9), 8.63 (d, J = 1.9 Hz, 2H, Phen-H4 and H7), 7.96 (s, 2H, Phen-H5 and H6), 7.56 (dd, J = 1.4, 8.0 Hz, 4H, Ph-H2 and H6), 7.33 (t, J = 8.0Hz, 4H, Ph-H3 and H5), 7.23 (tt, J = 1.4, 8.0 Hz, 2H, Ph-H4), 0.33 (s, 18H, ≡TMS).

2.4.2. Preparation of Pt(3,8-Phen≡TMS)(≡Ph-4-Me)$_2$ (**2**)

Pt(3,8-Phen≡TMS)(≡Ph-4-Me)$_2$ was synthesized by the same procedure to that for Pt(3,8-Phen≡TMS)(≡Ph)$_2$ except for the use of 1-ethynyl-4-methylbenzene (110 μl, 0.88 mmol). The red powder was obtained. Yield: 218 mg (68 %).
: Anal. Calcd for $C_{40}H_{38}N_2PtSi_2 \cdot 1/4CH_2Cl_2$: C, 59.0; H, 4.7; N, 3.4. Found: C, 59.2; H, 4.5; N, 3.3%. FT-IR (KBr,

cm^{-1}) ν(Pt-C≡C): 2116, ν(Phen-C≡C): 2162, ν(-CH_3): 2864, 2920, 2958. UV/VIS (CH_2Cl_2): λ_{abs} nm (ε × 10^{-5}) 237 (0.42), 267 (0.61), 283 (0.58), 323 (0.38), 342 (0.32), 358 (0.31), 472 (0.05). ^{1}H-NMR (CD_2Cl_2, 400MHz, ppm): δ = 10.01 (d, 2H, J = 1.7 Hz, Phen-H2 and H9), 8.63 (d, J = 1.7 Hz, 2H, Phen-H4 and H7), 7.96 (s, 2H, Phen-H5 and H6), 7.46 (d, J = 8.0 Hz, 4H, Ph-H2 and H6), 7.14 (d, J = 8.0 Hz, 4H, Ph-H3 and H5), 2.37 (s, 6H, Ph-CH_3), 0.34 (s, 18H, ≡TMS).

2.4.3. Preparation of Pt(3,8-Phen≡TMS)(≡Ph-4-*t*-Bu)$_2$ (**3**)

Pt(3,8-Phen≡TMS)(≡Ph-4-*t*-Bu)$_2$ was synthesized 3/4 scale by the same procedure to that for Pt(3,8-Phen≡TMS)(≡Ph)$_2$ except for the use of 1-ethynyl-4-*t*-butylbenzene (120 μl, 0.66 mmol). The residue was purified by SiO_2 chromatography with CH_2Cl_2/hexane (7:3) as eluent. The orange powder was obtained. Yield: 193 mg (72 %).
: Anal. Calcd for $C_{46}H_{50}N_2PtSi_2 \cdot 1/2CH_2Cl_2$: C, 60.4; H, 5.6; N, 3.0. Found: C, 60.2; H, 5.7; N, 2.9%. FT-IR (KBr, cm^{-1}) ν(Pt-C≡C): 2117, ν(Phen-C≡C): 2162, ν(-CH_3): 2867, 2900, 2960. UV/VIS (CH_2Cl_2): λ_{abs} nm (ε × 10^{-5}) 237 (0.45), 266 (0.66), 287 (0.63), 323 (0.40), 358 (0.32), 471 (0.06). ^{1}H-NMR (CD_2Cl_2, 400MHz, ppm): δ = 9.98 (d, J = 1.6 Hz, 2H, Phen-H2 and H9), 8.62 (d, J = 1.6 Hz, 2H, Phen-H4 and H7), 7.95 (s, 2H, Phen-H5 and H6), 7.50 (td, J = 2.0, 8.4 Hz, 4H, Ph-H2 and H6), 7.36 (td, J = 2.0, 8.4 Hz, 4H, Ph-H3 and H5), 1.35 (s, 18H, t-Bu)., 0.33 (s, 18H, ≡TMS).

2.4.4. Preparation of Pt(3,8-Phen≡TMS)(≡Ph-4-F)$_2$ (**4**)

Pt(3,8-Phen≡TMS)(≡Ph-4-F)$_2$ was synthesized by the same procedure to that for Pt(3,8-Phen≡TMS)(≡Ph)$_2$ except for the use of 1-ethynyl-4-fluorobenzene (100 μl, 0.88 mmol). The extracted residue was added small amounts of CH_3CN and filtered through the filter paper. The yellow powder was obtained. Yield: 292 mg (91 %).
: Anal. Calcd for $C_{38}H_{32}F_2N_2PtSi_2 \cdot 1/2CH_2Cl_2$: C, 54.5; H, 3.9; N, 3.3. Found: C, 54.6; H, 3.9; N, 3.3%. FT-IR (KBr, cm^{-1}) ν(Pt-C≡C): 2119, ν(Phen-C≡C): 2162, ν(-CH_3): 2900, 2959. UV/VIS (CH_2Cl_2): λ_{abs} nm (ε × 10^{-5}) 237 (0.48), 264 (0.63), 280 (0.61), 316 (0.39), 342 (0.37), 358 (0.36), 463 (0.06). ^{1}H-NMR (CD_2Cl_2, 400MHz, ppm): δ = 9.96 (d, J = 1.7 Hz, 2H, Phen-H2 and H9), 8.64 (d, J = 1.7 Hz, 2H, Phen-H4 and H7), 7.96 (s, 2H, Phen-H5 and H6), 7.53 (dd, J = 5.6, 8.8 Hz, 4H, Ph-H2 and H6), 7.02 (t, J = 8.8 Hz, 4H, Ph-H3 and H5), 0.33 (s, 18H, ≡TMS).

2.4.5. Preparation of Pt(3,8-Phen≡TMS)(≡Ph-3-F)$_2$ (**5**)

Pt(3,8-Phen≡TMS)(≡Ph-3-F)$_2$ was synthesized by the same procedure to that for Pt(3,8-Phen≡TMS)(≡Ph)$_2$ except for the use of 1-ethynyl-3-fluorobenzene (101 μl, 0.88 mmol). The residue was purified by SiO_2 chromatography with CH_2Cl_2/hexane (7:3) as eluent. The dark brown powder was obtained. Yield: 190 mg (59 %).
: Anal. Calcd for $C_{38}H_{32}F_2N_2PtSi_2 \cdot 1/2CH_2Cl_2$: C, 54.5; H, 3.9; N, 3.3. Found: C, 54.1; H, 3.9; N, 3.1%. FT-IR (KBr, cm^{-1}) ν(Pt-C≡C): 2116, ν(Phen-C≡C): 2162, ν(-CH_3): 2899, 2959. UV/VIS (CH_2Cl_2): λ_{abs} nm (ε × 10^{-5}) 237 (0.46),

266 (0.64), 280 (0.66), 342 (0.39), 359 (0.37), 453 (0.06). ^{1}H-NMR (CD_2Cl_2, 400MHz, ppm): δ = 9.84 (d, J = 2.0 Hz, 2H, Phen-H2 and H9), 8.61 (d, J = 2.0 Hz, 2H, Phen-H4 and H7), 7.94 (s, 2H, Phen-H5 and H6), 7.30 (d, J = 8.0 Hz, 2H, Ph-H6), 7.28 (dd, J = 2.0, 8.0 Hz, 2H, Ph-H5), 7.22 (m, 2H, Ph-H2), 6.94 (m, 2H, Ph-H4), 0.33 (s, 18H, ≡TMS).

2.4.6. Preparation of Pt(3,8-Phen≡TMS)(≡Ph-2-F)$_2$ (**6**)

Pt(3,8-Phen≡TMS)(≡Ph-2-F)$_2$ was synthesized by the same procedure to that for Pt(3,8-Phen≡TMS)(≡Ph)$_2$ except for the use of 1-ethynyl-2-fluorobenzene (100 μl, 0.88 mmol). The orange powder was obtained. Yield: 216 mg (67 %).

: Anal. Calcd for $C_{38}H_{32}F_2N_2PtSi_2 \cdot C_4H_{10}O_1$: C, 57.3; H, 4.8; N, 3.2. Found: C, 57.3; H, 4.8; N, 2.8%. FT-IR (KBr, cm^{-1}) ν(Pt-C≡C): 2125, ν(Phen-C≡C): 2163, ν(-CH_3): 2958. UV/VIS (CH_2Cl_2): λ_{abs} nm (ε × 10^{-5}) 237 (0.43), 264 (0.59), 280 (0.60), 304 (0.48), 313 (0.48), 342 (0.37), 360 (0.36), 455 (0.06). ^{1}H-NMR (CD_2Cl_2, 400MHz, ppm): δ = 10.02 (d, J = 1.6 Hz, 2H, Phen-H2 and H9), 8.58 (d, J = 1.6 Hz, 2H, Phen-H4 and H7), 7.94 (s, 2H, Phen-H5 and H6), 7.57 (td, J = 1.6, 7.6 Hz, 2H, Ph-H3), 7.22 (tdd, J = 1.6, 5.2, 7.8 Hz, 2H, Ph-H5), 7.14 (dd, J = 1.0, 7.8 Hz, 2H, Ph-H6), 7.11 (m, 2H, Ph-H4), 0.35 (s, 18H, ≡TMS).

2.4.7. Preparation of Pt(3,8-Phen≡TMS)(≡Ph-3,5-t-Bu)$_2$ (**7**)

Pt(3,8-Phen≡TMS)(≡Ph-3,5-*t*-Bu)$_2$ was synthesized 3/4 scale by the same procedure to that for Pt(3,8-Phen≡TMS)(≡Ph)$_2$ except for the use of 1-ethynyl-3,5-di-*t*-butyl-benzene (150 mg, 0.70 mmol). The brown red powder was obtained. Yield: 265 mg (88 %).

: Anal. Calcd for $C_{54}H_{66}N_2PtSi_2$: C, 65.2; H, 6.7; N, 2.8. Found: C, 65.2; H, 6.9; N, 2.7%. FT-IR (KBr, cm^{-1}) ν(Pt-C≡C): 2110, ν(Phen-C≡C): 2160, ν(-CH_3): 2868, 2902, 2962. UV/VIS (CH_2Cl_2): λ_{abs} nm (ε × 10^{-5}) 234 (0.51), 267 (0.62), 283 (0.59), 323 (0.38), 340 (0.33), 357 (0.32), 473 (0.05). ^{1}H-NMR (CD_2Cl_2, 400MHz, ppm): δ = 9.99 (d, J = 1.8 Hz, 2H, Phen-H2 and H9), 8.70 (d, J = 1.8 Hz, 2H, Phen-H4 and H7), 7.98 (s, 2H, Phen-H5 and H6), 7.45 (d, J = 1.8 Hz, 4H, Ph-H2 and H6), 7.30 (t, J = 1.8 Hz, 2H, Ph-H4), 1.37 (s, 36H, t-Bu), 0.30 (s, 18H, ≡TMS).

2.4.8. Preparation of Pt(3,8-Phen≡TMS)(≡Ph-4-CF_3)$_2$ (**8**)

Pt(3,8-Phen≡TMS)(≡Ph-4-CF_3)$_2$ was synthesized 3/4 scale by the same procedure to that for Pt(3,8-Phen≡TMS)(≡Ph)$_2$ except for the use of 1-ethynyl-4-trifluoromethyl-benzene (110 μl, 0.66 mmol). The extracted residue was added small amounts of CH_3CN and filtered through the filter paper. The brown powder was obtained. Yield: 245 mg (90 %).

: Anal. Calcd for $C_{40}H_{32}F_6N_2PtSi_2$: C, 53.0; H, 3.6; N, 3.1. Found: C, 53.0; H, 3.7; N, 3.0%. FT-IR (KBr, cm^{-1}) ν(-CF_3): 1120, 1163, ν(Pt-C≡C): 2117, ν(Phen-C≡C): 2162, ν(-CH_3): 2901, 2961. UV/VIS (CH_2Cl_2): λ_{abs} nm (ε × 10^{-5}) 237 (0.44), 280 (0.72), 290 (0.71), 313 (0.55), 340 (0.39), 360 (0.38), 451 (0.07). ^{1}H-NMR (CD_2Cl_2, 400MHz, ppm):

δ = 9.85 (d, J = 1.0 Hz, 2H, Phen-H2 and H9), 8.62 (d, J = 1.0 Hz, 2H, Phen-H4 and H7), 7.94 (s, 2H, Phen-H5 and H6), 7.63 (d, J = 8.4 Hz, 4H, Ph-H2 and H6), 7.56 (d, J = 8.4 Hz, 4H, Ph-H3 and H5), 0.32 (s, 18H, ≡TMS).

2.4.9. Preparation of Pt(3,8-Phen≡TMS)(≡Ph-3,5-CF_3)$_2$ (**9**)

Pt(3,8-Phen≡TMS)(≡Ph-3,5-CF_3)$_2$ was synthesized 3/4 scale by the same procedure to that for Pt(3,8-Phen≡TMS)(≡Ph)$_2$ except for the use of 1-ethynyl-3,5-bis(trifluoromethyl)-benzene (117 μl, 0.66 mmol). The extracted residue was added small amounts of Et_2O and filtered through the filter paper. The brown powder was obtained. Yield: 269 mg (86 %).

: Anal. Calcd for $C_{42}H_{30}F_{12}N_2PtSi_2$: C, 48.4; H, 2.9; N, 2.7. Found: C, 48.5; H, 3.2; N, 2.6%. FT-IR (KBr, cm^{-1}) ν(-CF_3): 1132, 1181, ν(Pt-C≡C): 2112, ν(Phen-C≡C): 2144, ν(-CH_3): 2963. UV/VIS (CH_2Cl_2): λ_{abs} nm (ε × 10^{-5}) 237 (0.40), 278 (0.67), 289 (0.63), 340 (0.36), 360 (0.36), 441 (0.06). ^{1}H-NMR (CD_2Cl_2, 400MHz, ppm): δ = 9.86 (d, J = 1.6 Hz, 2H, Phen-H2 and H9), 8.71 (d, J = 1.6 Hz, 2H, Phen-H4 and H7), 8.00 (s, 6H, Phen-H5 and H6, Ph-H2 and H6), 7.71 (s, 2H, Ph-H4), 0.29 (s, 18H, ≡TMS).

2.4.10. Preparation of Pt(3,8-Phen≡TMS)(≡Ph-4-COOMe)$_2$ (**10**)

Pt(3,8-Phen≡TMS)(≡Ph-4-COOMe)$_2$ was synthesized 3/4 scale by the same procedure to that for Pt(3,8-Phen≡TMS)(≡Ph)$_2$ except for the use of 1-ethynyl-4-methylcarboxy-benzene (106 mg, 0.66 mmol). The dark red powder was obtained. Yield: 194 mg (73 %).

: Anal. Calcd for $C_{42}H_{38}N_2O_4PtSi_2 \cdot 1/2C_4H_{10}O_1$: C, 57.3; H, 4.7; N, 3.0. Found: C, 57.3; H, 4.8; N, 2.9%. FT-IR (KBr, cm^{-1}) ν(C=O): 1718, ν(Pt-C≡C): 2114, ν(Phen-C≡C): 2163, ν(-CH_3): 2900, 2953. UV/VIS (CH_2Cl_2): λ_{abs} nm (ε × 10^{-5}) 236 (0.44), 282 (0.56), 292 (0.58), 326 (0.75), 361 (0.33), 452 (0.06). ^{1}H-NMR (CD_2Cl_2, 400MHz, ppm): δ = 9.85 (d, J = 1.8 Hz, 2H, Phen-H2 and H9), 8.61 (d, J = 1.8 Hz, 2H, Phen-H4 and H7), 7.96 (d, J = 8.6 Hz, 4H, Ph-H3 and H5), 7.93 (s, 2H, Phen-H5 and H6), 7.57 (d, J = 8.6 Hz, 4H, Ph-H2 and H6), 3.90 (s, 6H, -$COOCH_3$), 0.33(s, 18H, ≡TMS).

2.4.11. Preparation of Pt(3,8-Phen≡TMS)(≡Ph-4-NO_2)$_2$ (**11**)

Pt(3,8-Phen≡TMS)(≡Ph-4-NO_2)$_2$ was synthesized 3/4 scale by the same procedure to that for Pt(3,8-Phen≡TMS)(≡Ph)$_2$ except for the use of 1-ethynyl-4-nitro-benzene (98 mg, 0.66 mmol). The black powder was obtained. Yield: 188 mg (72 %).

: Anal. Calcd for $C_{38}H_{32}N_4O_4PtSi_2 \cdot 1/4CH_2Cl_2$: C, 52.1; H, 3.7; N, 6.4. Found: C, 51.9; H, 3.7; N, 6.2%. FT-IR (KBr, cm^{-1}) ν(-NO_2): 1337, ν(Pt-C≡C): 2112, ν(Phen-C≡C): 2162, ν(-CH_3): 2917, 2960. UV/VIS (CH_2Cl_2): λ_{abs} nm (ε × 10^{-5}) 237 (0.51), 279 (0.45), 343 (0.66), 361 (0.73), 440 (0.09). ^{1}H-NMR (CD_2Cl_2, 400MHz, ppm): δ = 9.92 (d, J = 1.7 Hz, 2H, Phen-H2 and H9), 8.70 (d, J = 1.7 Hz, 2H, Phen-H4 and H7), 8.17 (d, J = 8.6 Hz, 4H, Ph-H3 and H5),

8.01 (s, 2H, Phen-H5 and H6), 7.63 (d, J = 8.6 Hz, 4H, Ph-H2 and H6), 0.32 (s, 18H, ≡TMS).

3. Results and discussion

3.1. Synthesis and characterization of platinum complexes

The ligand of 3,8-Phen≡TMS was synthesized by a Sonogashira coupling reaction in good yields as previously reported [24]. Eleven new platinum phenanthroline organometallic complexes **1 - 11** with respective arylethynyl ligands with different substituents (**Pt(3,8-Phen≡TMS)(≡Ph-R)$_2$**: **R** = H (**1**), 4-Me (**2**), 4-*t*-Bu (**3**), 4-F (**4**), 3-F (**5**), 2-F (**6**), 3,5-di-*t*-Bu (**7**), 4-CF_3 (**8**), 3,5-di-CF_3 (**9**), 4-COOMe (**10**), and 4-NO_2 (**11**)) were synthesized with an excess DIEA and 5% copper iodide for transmetalation reaction (Scheme 1). These 11 substituents were included in the electron donating group, such as alkyl substituents, and in the electron withdrawing group, such as nitro and methyl carboxyl substituents, as shown in Scheme 1. All complexes were characterized by IR, ^{1}H-NMR, UV-Vis, luminescence spectroscopy, and elemental analysis. All of the new platinum organometallics exhibited ^{1}H-NMR signals and elemental analysis results in accordance with the assigned structures presented in Scheme 1.

The IR spectra of these complexes indicated that the η^1 coordination of metal−carbon bonds between the Pt atom and the ethynyl functional group of each of the 11 arylethynyl ligands. The characteristic strong ν(C≡C) bands assigned to the Pt-C≡C bond of the present platinum complexes were observed at around 2110 cm^{-1} (among 2110-2125 cm^{-1}) except for platinum complex **9**, which had two peaks, at 2112 and 2144 cm^{-1}. Furthermore, the ν(C≡C) peak of the Pt–C≡C bond is almost consistent with that (2113 cm^{-1}) of the previously reported platinum complex Pt(3,8-bis-pyridylethynyl-phenanthroline)(-≡-$C_6H_5CH_3$)$_2$ [26]. In addition, a weak ν(C≡C) band assigned to the trimethylsilyl−ethynyl substituent in the phenanthroline ligand was observed at 2162 cm^{-1} (among 2160-2163 cm^{-1}), although the peak of **9** was not confirmed because it overlapped with the strong peak at 2144 cm^{-1}, as mentioned above. The lack of a peak for ν(C≡C-H) observed at around 3300 cm^{-1} in the IR spectra of all complexes

The formation of the Pt–C≡C bond is supported by the ^{1}H-NMR measurements. No assignable signal for the ethynyl proton of any of the arylethynyl ligands in the ^{1}H-NMR spectra of all complexes was detected. The signals assignable to the phenanthroline-H2 and -H9 protons on the platinum complexes clearly showed downfield shifts of more than 0.5 ppm compared with the signal of the free 3,8-Phen≡TMS ligand. The phenomenon of the downfield shift is also consistent with the results for our previously reported complex Pt(3,8-bis-pyridylethynyl-phenanthroline)(-≡-$C_6H_4CH_3$)$_2$ [26].

3.2. Photophysical data on platinum complexes

Figures 1 and 2 show the absorption spectra of platinum organometallics **1-11** and two related compounds in CH_2Cl_2. These platinum organometallics with 11 arylethynyl ligands each have a broad absorption band over 400

nm, and this band was primarily assigned to the mixed transition of both the MLCT from platinum ion to 3,8-Phen≡TMS and the LLCT from the respective arylethynyl ligands to the 3,8-Phen≡TMS phenanthroline ligand. The absorption bands of these complexes in the 340-370 nm region, as shown in Fig. 1, were primarily assigned to the lowest π-π*(3,8-Phen≡TMS) singlet transition because the bands assignable to the lowest energy π-π*(3,8-Phen≡TMS) transition of Pt(3,8-Phen≡TMS)Cl_2 are observed in the same wavelength area shown in Fig. 2 and because the spectrum of Pt(dppp)(-≡-C_6H_5)$_2$ (dppp = 1,3-bis(diphenyphosphino)propane) showed no absorption band over the 340 nm region (Fig. 2). The spectra of both complexes **10** and **11** overlapped with the lowest π-π*(3,8-Phen≡TMS) and π-π*(-≡-C_6H_4R) transition bands of the respective arylethynyl ligands with carboxy methyl ester (**10**) and nitro substituents (**11**) at the para position in the 330-380 nm region (Fig. 2). These findings are consistent with those of previous reports on similar platinum(II) complexes with bipyridine derivatives [20, 22]. The band of the mixed transition from MLCT and LLCT, namely ^{1}MLCT/^{1}LLCT, over 400 nm in these platinum organometallics confirmed a hypsochromic effect of the present arylethynyl ligands in these organometallics. Complexes **11** and **9** with nitro and bis-trifluoromethyl substituents as electron-withdrawing groups each exhibited an absorption band of ^{1}MLCT/^{1}LLCT in the short wavelength area compared to the band of the same transition in **2** and **3** with methyl and *t*-butyl substituents as electron-donating groups, although the peaks of the bands are not clear because of the breadth of the band.

The platinum complexes showed a visible broad emission band in deoxygenated CH_2Cl_2 at room temperature upon excitation at 425 nm, while complexes **9** and **11** showed a high-intensity emission band with small vibronic progressions in the high-energy region (Fig. 3). The present organometallics in 2-MeTHF at 77 k also showed emission with clear vibronic progressions upon excitation at 425 nm (Fig. 4). These emissions are also assigned to phosphorescence from the triplet state of the mixed transition from MLCT and LLCT, namely ^{3}MLCT/^{3}LLCT, which is well known to be present in the luminescence for similar platinum(II) organometallic complexes with bipyridine derivatives and two various arylethynyl ligands, Pt(L)(≡-aryl)$_2$ and (L = bipyridine derivatives) [10-19].

The maximum intensity peaks of the emission band (λ_{em}) at room temperature in deoxygenated CH_2Cl_2 and those at 77 K in deoxygenated 2-MeTHF for the present platinum complexes **1-11** are collected in Table 1. The peak wavelength values show that the complexes with the electron-withdrawing group are smaller, which are higher-energy values, than those with the electron-donating group. This trend is consistent with the tendency of the mixed transition of ^{1}MLCT/^{1}LLCT to express less ambiguous evidence in UV-Vis spectra. The values at room temperature span a wide range, 540-655 nm, while those at 77 k are in a narrower region, 518-568 nm. This difference might be related to the emission with the mixed transition of ^{3}MLCT/^{3}LLCT. The emission quantum yields (ϕ_{em}) at room temperature calculated by the standard relative method [21] are also listed in Table 1. Interestingly, ϕ_{em} increased with decreasing λ_{em} from 655 nm to 570 nm for **1-11**. This result could be assumed to be caused by the so-called energy gap law because present platinum complexes **1-11** as shown in Scheme 1 were

very similar structures.

The present organometallics each have a broad lowest energy absorption band assigned to the mixed transition of both ^{1}MLCT and ^{1}LLCT to 3,8-Phen≡TMS, and this absorption band was confirmed to have a hypsochromic effect among the present arylethynyl ligands; bands in the organometallics with an electron-withdrawing group were observed in the short wavelength area compared to those in the compounds with an electron-donating group. The emission bands in the present organometallics were assigned to the phosphorescence of ^{3}MLCT/^{3}LLCT, and the trend of the maximum peak wavelength was also consistent with the tendency of the absorption bands mentioned above. This trend of photophysical data of present organometallics is strongly related to the HOMOs mixed both metal d orbitals and π orbitals on respective arylethynyl ligands in their complexes and discussed in next section.

3.3. DFT and TD-DFT calculations of platinum complexes

DFT and TD-DFT calculations of all organometallics aid the interpretation of the electronic effects of their aryl groups with different substituents on phosphorescence in CH_2Cl_2 at room temperature. Under the singlet ground (S_0) state, the MO energy levels and spatial plots of the MOs at the HOMO and LUMO calculated in CH_2Cl_2 solution with the PCM method by DFT are shown in Fig. 5. The HOMOs of their complexes show the electron distributions mixed both metal d orbitals and π orbitals on respective arylethynyl ligands, while the LUMOs of them mainly show the electron distributions of π^* orbitals on the diethynylphenanthroline skeleton of the 3,8-Phen≡TMS ligand. These results are consistent with the assignment to the mixed transition of both MLCT from platinum ion to 3,8-Phen≡TMS and LLCT from respective arylethynyl ligands to the 3,8-Phen≡TMS for the lowest energy transition in the UV-Vis spectra of the present complexes. The maximum difference (0.62 eV) of the HOMOs for the 11 platinum compounds (CH_3 substituent, -5.24 eV; NO_2 substituent, -5.86 eV) is greater than the difference (0.16 eV) of the LUMOs for these compounds (CH_3 substituent, -2.79 eV; NO_2 substituent, -2.95 eV), as shown in Fig. 5. The difference between HOMO and LUMO in respective complexes supports the idea that the lowest transition energy could be predominantly tuned with the arylethynyl ligands of the present platinum(II) organometallics, and the effects of the different arylethynyl ligands could be estimated by DFT calculation because the trend in the energy difference is consistent with the tendency toward the mixed transition bands of ^{1}MLCT/^{1}LLCT in UV-Vis spectra.

An interesting finding is the good linear correlation between the emission energy values of the maximum intensity peak in the phosphorescent band, E_{em}, and the $E(T_1\text{-}S_0)_{DFT}$ or $E(T_1\text{-}S_0)_{TD\text{-}DFT}$ in terms of eV as shown in Figure 6. The energy separation, $E(T_1\text{-}S_0)_{DFT}$, between the excited triplet (T_1) state and the S_0 state decreased the HOMO energy level under the S_0 state from the highest SOMO under the T_1 state, while the value of the direct T_1-S_0 transition energy, $E(T_1\text{-}S_0)_{TD\text{-}DFT}$, was obtained from the TD-DFT calculation in CH_2Cl_2. The calculated results of

$E(T_1\text{-}S_0)_{DFT}$ and $E(T_1\text{-}S_0)_{TD\text{-}DFT}$ also are collected in Table 1. This linear correlation between the observed emission data and the calculated results by DFT and TD-DFT precisely underscores that the related MOs obtained by these calculations reflect the actual MOs in the present organometallics.

4. Conclusion

Platinum(II) phenanthroline organometallic complexes Pt(3,8-Phen≡TMS)(≡Ph-R)$_2$ of respective arylethynyl ligands with different substituents (R = H (**1**), 4-Me (**2**), 4-*t*-Bu (**3**), 4-F (**4**), 3-F (**5**), 2-F (**6**), 3,5-di-*t*-Bu (**7**), 4-CF_3 (**8**), 3,5-di-CF_3 (**9**), 4-COOMe (**10**), and 4-NO_2 (**11**)) were synthesized by transmetalation reaction with copper(I) ion. The present organometallics each have a broad absorption band assigned to the mixed transition of both ^{1}MLCT and ^{1}LLCT to 3,8-Phen≡TMS over 400 nm, and this absorption band was confirmed to have a hypsochromic effect among the present arylethynyl ligands; bands in the organometallics with an electron-withdrawing group were observed in the short wavelength area compared to those in the compounds with an electron-donating group. The emission bands in the present organometallics were assigned to the phosphorescence of ^{3}MLCT/^{3}LLCT, and the trend of the maximum peak wavelength was also consistent with the tendency of the absorption bands of both ^{1}MLCT/^{1}LLCT mentioned above.

DFT and TD-DFT calculations of all 11 organometallics clearly supported the assignment of phosphorescence in these compounds. A good linear correlation between the emission energy values of phosphorescence, E_{em}, and the calculation values, $E(T_1\text{-}S_0)_{DFT}$ or $E(T_1\text{-}S_0)_{TD\text{-}DFT}$, by DFT and TD-DFT reflects that the related MOs of these complexes are included in both MLCT and LLCT under a photo-excited state.

We are currently extending our photophysical research to study the solid state emission and vapochromism of the present platinum organometallics.

Acknowledgements

This work was supported in part by JSPS KAKENHI Grant Number 23550074 from Japan Society for the Promotion of Science, Japan.

References

[1] (a) K.T. Ly, R.-W. Chen-Cheng, H.-W. Lin, Y.-J. Shiau, S.-H. Liu P.-T. Chou, C.-S. Tsao, Y.-C. Huang, Y. Chi, Near-infrared organic light-emitting diodes with very high external quantum efficiency and radiance, Nat. Photonics. 11 (2016) 63-68;

(b) P. Mahato, A. Monguzzi, N. Yanai, T. Yamada, N. Kimizuka, Fast and long-range triplet exciton diffusion in metal–organic frameworks for photon upconversion at ultralow excitation power, Nat. Mater. 14 (2015) 924-930;

(c) X. Yan, T.R. Cook, P. Wang, F. Huang, P.J. Stang, Highly emissive platinum(II) metallacages Nat. Chem. 7 (2015) 342-348.

[2] (a) F.K.-W. Kong, M.-C. Tang, Y.-C. Wong, M.-Y. Chan, V.W.-W. Yam, Design Strategy for High-Performance Dendritic Carbazole-Containing Alkynylplatinum(II) Complexes and Their Application in Solution-Processable Organic Light-Emitting Devices, J. Am. Chem. Soc. 138 (2016) 6281-6291;

(b) K. Li, G. S.M. Tong, Q. Wan, G. Cheng, W.-Y. Tong, W.-H. Ang, W.-L. Kwong, C.-M. Che, Highly phosphorescent platinum(II) emitters: photophysics, materials and biological applications, Chem. Sci. 7 (2016) 1653-1673.

[3] (a) C.-L. Ho, Z.-Q. Yu W.-Y. Wong, Multifunctional polymetallaynes: properties, functions and applications, Chem. Soc. Rev. 45 (2016) 5264;

(b) C.-L. Ho, W.-Y. Wong, Charge and energy transfers in functional metallophosphors and metallopolyynes, Coord. Chem. Rev. 257 (2013) 1614;

(c) C.-L. Ho, W.-Y. Wong, Metal-containing polymers: Facile tuning of photophysical traits and emerging applications in organic electronics and photonics, Coord. Chem. Rev. 255 (2011) 2469;

(d) W.-Y. Wong, C.-L. Ho, Di-, oligo- and polymetallaynes: Syntheses, photophysics, structures and applications, Coord. Chem. Rev. 250 (2006) 2627;

(e) W.-Y. Wong, C.-L. Ho, Heavy metal organometallic electrophosphors derived from multi-component chromophores, Coord. Chem. Rev. 253 (2009) 1709.

[4] (a) W.-Y. Wong, P.D. Harvey, Recent Progress on the Photonic Properties of Conjugated Organometallic Polymers Built Upon the trans-Bis(para-ethynylbenzene)bis(phosphine)platinum(II) Chromophore and Related Derivatives, Macromol. Rapid Commun. 31 (2010) 671;

(b) W.-Y. Wong, Luminescent organometallic poly(aryleneethynylene)s: functional properties towards implications in molecular optoelectronics, Dalton Trans. 2007, 4495;

(c) G.-J. Zhou, W-Y. Wong, Organometallic acetylides of PtII, AuI and HgII as new generation optical power limiting materials, Chem. Soc. Rev. 40 (2011) 2541;

(d) W.-Y. Wong, C.-L. Ho, Organometallic Photovoltaics: A New and Versatile Approach for Harvesting Solar

Energy Using Conjugated Polymetallaynes, Acc. Chem. Res. 43 (2010) 1246.
[5] (a) J. Xiang, C.-L. Ho, W.-Y. Wong, Metallopolymers for energy production, storage and conservation, Polym. Chem. 6 (2015) 6905;
(b) X. Yang, G. Zhou, W.-Y. Wong, Functionalization of phosphorescent emitters and their host materials by main-group elements for phosphorescent organic light-emitting devices, Chem. Soc. Rev. 44 (2015) 8484;
(c) C.-L. Ho, H. Li, W.-Y. Wong, Red to near-infrared organometallic phosphorescent dyes for OLED applications, J. Organomet. Chem. 751 (2014) 261;
(d) C.-L. Ho, W.-Y. Wong, Small-molecular blue phosphorescent dyes for organic light-emitting devices, New J. Chem. 37 (2013) 1665;
(e) W.-Y. Wong, C.-L. Ho, Functional metallophosphors for effective charge carrier injection/transport: new robust OLED materials with emerging applications, J. Mater. Chem. 19 (2009) 4457.
[6] (a) S. Campagna, F. Puntoriero, F. Nastasi, G. Bergamini, V. Balzani, Photochemistry and Photophysics of Coordination Compounds: Ruthenium, Top. Curr. Chem. 280 (2007) 117-214;
(b) J.A.G. Williams, Photochemistry and Photophysics of Coordination Compounds: Platinum, Top. Curr. Chem. 257 (2005) 1-32;
(c) V.W.-W. Yam, K.M.-C. Wong, Luminescent Molecular Rods-transition-Metal Alkynyl Complexes, Top. Curr. Chem. 281 (2007) 205-268.
[7](a) W. Yang, J. Zhao, Photophysical Properties of Visible-Light-Harvesting PtII Bis(acetylide) Complexes, Eur. J. Inorg. Chem. 2016 (2016) 5283;
(b) M. Delor, S.A. Archer, T. Keane, A.J.H.M. Meijer, I.V. Sazanovich, G.M. Greetham, M. Towrie, J.A. Weinstein, Directing the path of light-induced electron transfer at a molecular fork using vibrational excitation, Nat. Chem. doi:10.1038/nchem.2793.
[8] (a) J.E. McGarrah, R. Eisenberg, Dyads for Photoinduced Charge Separation Based on Platinum Diimine Bis(acetylide) Chromophores: Synthesis, Luminescence and Transient Absorption Studies, Inorg. Chem. 42 (2003) 4355;
(b) E.A. Glik, S. Kinayyigit, K.L. Ronayne, M. Towrie, I.V. Sazanovich, J.A. Weinstein, F.N. Castellano, Ultrafast Excited State Dynamics of Pt(II) Chromophores Bearing Multiple Infrared Absorbers, Inorg. Chem. 47 (2008) 6974;
(c) F. Zhong, A. Karatay, L. Zhao, J. Zhao, C. He, C. Zhang, H.G. Yaglioglu, A. Elmali, B. Küçüköz, M. Hayvali, Broad-Band N∧N Pt(II) Bisacetylide Visible Light Harvesting Complex with Heteroleptic Bodipy Acetylide Ligands, Inorg. Chem. 54 (2015) 7803;
(d) P.-Y. Ho, B. Zheng, D. Mark, W.-Y. Wong, D.W. McCamant, R. Eisenberg, Chromophoric Dyads for the Light-Driven Generation of Hydrogen: Investigation of Factors in the Design of Multicomponent Photosensitizers for

Proton Reduction, Inorg. Chem. 55 (2016) 8348.

[9] A. Julis, V. Balzani, F. Baligelletti, S. Campagna, P. Belser, A.V. Zelewsky, Ru(II) polypyridine complexes: Photophysics, photochemistry, electrochemistry, and chemiluminescence, Coord. Chem. Rev. 84 (1988) 85-277.

[10] J. Ni, Y.-G. Wang, H.-H. Wang, Y.-Z. Pan, L. Xu, Y.-Q. Zhao, X.-Y. Liu, J.-J. Zhang, Reversible Dual-Stimulus-Responsive Luminescence and Color Switch of a Platinum Complex with 4-[(2-Trimethylsilyl)ethynyl]-2,2′-bipyridine, Eur. J. Inorg. Chem. 2014 (2014) 986-993.

[11] J. Ni, Y.-G. Wang, J.-Y. Wang, Y.-Q. Zhao, Y.-Z. Pan, H.-H. Wang, X. Zhang, J.-J. Zhanga, Z.-N. Chen, A new sensor for detection of CH_3CN and $ClCH_2CN$ vapors based on vapoluminescent platinum(II) complex, Dalton Trans. 42 (2013) 13092-13100.

[12] X. Zhang, J.-Y. Wang, J. Ni, L.-Y. Zhang, Z.-N. Chen, Vapochromic and Mechanochromic Phosphorescence Materials Based on a Platinum(II) Complex with 4-Trifluoromethylphenylacetylide, Inorg. Chem. 51 (2012) 5569-5579.

[13] J. Ni, X. Zhang, Y.-H. Wu, L.-Y. Zhang, Z.-N. Chen, Vapor- and Mechanical-Grinding-Triggered Color and Luminescence Switches for Bis(σ-fluorophenylacetylide) Platinum(II) Complexes, Chem. Eur. J. 17 (2011) 1171-1183.

[14] J. Ni, X. Zhang, N. Qiu, Y.-H. Wu, L.-Y. Zhang, J. Zhang, Z.-N. Chen, Mechanochromic Luminescence Switch of Platinum(II) Complexes with 5-Trimethylsilylethynyl-2,2-bipyridine, Inorg. Chem. 50 (2012) 9090-9096.

[15] J. Ni, L.-Y. Zhang, H.-M. Wena, Z.-N. Chen, Luminescence vapochromic properties of a platinum(II) complex with 5,5'-bis(trimethylsilylethynyl)-2,2'-bipyridine, Chem. Commun. 25 (2009) 3801-3803.

[16] J. Ni, Y.-H. Wu, X. Zhang, B. Li, L.-Y. Zhang, Z.-N. Chen, Luminescence Vapochromism of a Platinum(II) Complex for Detection of Low Molecular Weight Halohydrocarbon, Inorg. Chem. 48 (2008) 10202-10210.

[17] Z. M. Hudson, C. Sun, K. J. Harris, B. E. G. Lucier, R. W. Schurko, S. Wang, Probing the Structural Origins of Vapochromism of a Triarylboron-Functionalized Platinum(II) Acetylide by Optical and Multinuclear Solid-State NMR Spectroscopy, Inorg. Chem. 50 (2011) 3447-3457.

[18] K.-C.Chang, J.-L. Lin, Y.-T. Shen, C.-Y. Hung, C.-Y. Chen, S.-S. Sun, Synthesis and Photophysical Properties of Self-Assembled Metallogels of Platinum(II) Acetylide Complexes with Elaborate Long-Chain Pyridine-2,6-Dicarboxamides, Chem. Eur. J. 18 (2012) 1312-1321.

[19] Y. Li, A. Y.-Y. Tam, K. M.-C. Wong, W. Li, L. Wu, V. W.-W. Yam, Synthesis, Characterization, and the Photochromic, Luminescence, Metallogelation and Liquid-Crystalline Properties of Multifunctional Platinum(II) Bipyridine Complexes, Chem. Eur. J. 17 (2011) 8048-8059.

[20] M. Hissler, W. B. Connick, D.K. Geiger, J. E. McGarrah, D. Lipa, R.J. Lachicotte, R. Eisenberg, Platinum Diimine Bis(acetylide) Complexes: Synthesis, Characterization, and Luminescence Properties, Inorg. Chem. 39 (2000) 447-457.

[21] S.-C. Chan, M.C.W. Chan, Y. Wang, C.-M. Che, K.-K. Cheung, N. Zhu, Organic light-emitting materials based on bis(arylacetylide)platinum(II) complexes bearing substituted bipyridine and phenanthroline ligands: photo- and electroluminescence from ^{3}MLCT excited states, Chem. Eur. J. 7 (2001) 4180-4190.
[22] C.E. Whittle, J.A. Weinstein, M.W. George, K.S. Schanze, Photophysics of Diimine Platinum(II) Bis-Acetylide Complexes, Inorg. Chem. 40 (2001) 4053-4062.
[23] W. Lu, M.C.W. Chan, N. Zhu, C.-M. Che, Z. He, K.-Y. Wong, Structural Basis for Vapoluminescent Organoplatinum Materials Derived from Noncovalent Interactions as Recognition Components, Chem. Eur. J. 9 (2003) 6155-6166.
[24] R. Ziessel, C. Stroh, Segmented multitopic ligands constructed from bipyrimidine, phenanthroline, and terpyridine modules, Tetrahedron Lett. 45 (2004) 4051-4055.
[25] M.J. Frisch et al., Gaussian 09W, revision C.01; Gaussian Inc.: Wallingford, CT, 2009.
[26] M. Shiotsuka, Y. Ueno, D. Asano, T. Matsuoka, K. Sako, Synthesis and photophysical characterization of ruthenium(II) and platinum(II) complexes with bis-pyridylethynyl-phenanthroline ligands as a metalloligand, Transition Met. 40 (2015) 673-679.

Scheme 1. Molecular structures of new platinum organometallics, Pt(3,8-Phen≡TMS)(≡aryl)$_2$, **1** - **11**.

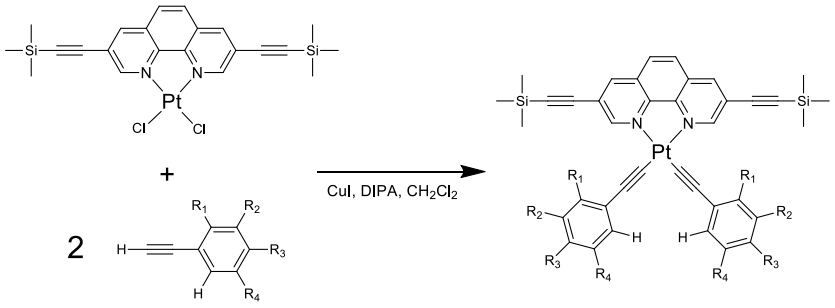

1: H = R_1, R_2, R_3, R_4
2: CH_3 = R_3; H = R_1, R_2, R_4
3: $C(CH_3)_3$ = R_3; H = R_1, R_2, R_4
4: F = R_3; H = R_1, R_2, R_4
5: F = R_2; H = R_1, R_3, R_4
6: F = R_1; H = R_2, R_3, R_4
7: $C(CH_3)_3$ = R_2, R_4; H = R_1, R_3
8: CF_3 = R_3; H = R_1, R_2, R_4
9: CF_3 = R_2, R_4; H = R_1, R_3
10: COOMe = R_3; H = R_1, R_2, R_4
11: NO_2 = R_3; H = R_1, R_2, R_4

Table 1. Luminescence data and emission energy calculated by DFT and TD-DFT of platinum organometallics **1** - **11**.

Compound	Emission				DFT and TD-DFT data	
	λ_{em} /nm at r.t.	λ_{em} / nm at 77 K	ϕ_{em}[a] / % at r.t.	E_{em}[b] / eV at r.t.	$E(T_1\text{-}S_0)_{DFT}$ (eV)	$E(T_1\text{-}S_0)_{TD\text{-}DFT}$ (eV)
1	624	551	7.4	1.99	1.80	1.95
2	655	568	2.1	1.89	1.73	1.87
3	651	566	2.6	1.90	1.74	1.88
4	628	549	5.0	1.97	1.79	1.94
5	599	536	21.6	2.07	1.89	2.06
6	601	538	14.4	2.06	1.89	2.06
7	650	566	2.5	1.91	1.75	1.89
8	580	525	34.8	2.14	1.95	2.12
9	540	518	42.7	2.30	1.98	2.20
10	586	530	32.9	2.12	1.94	2.10
11	548	523	42.0	2.26	2.03	2.15

[a] Emission quantum yields (ϕ_{em}) were calculated relative to $[Ru(bpy)_3](PF_6)_2$ in a degassed acetonitrile (ϕ_{em} = 0.095) as a standard.
[b] Wavelengths of emission maxima are converted to eV ($E_{em} = 1240/\lambda_{em}$).

Figures

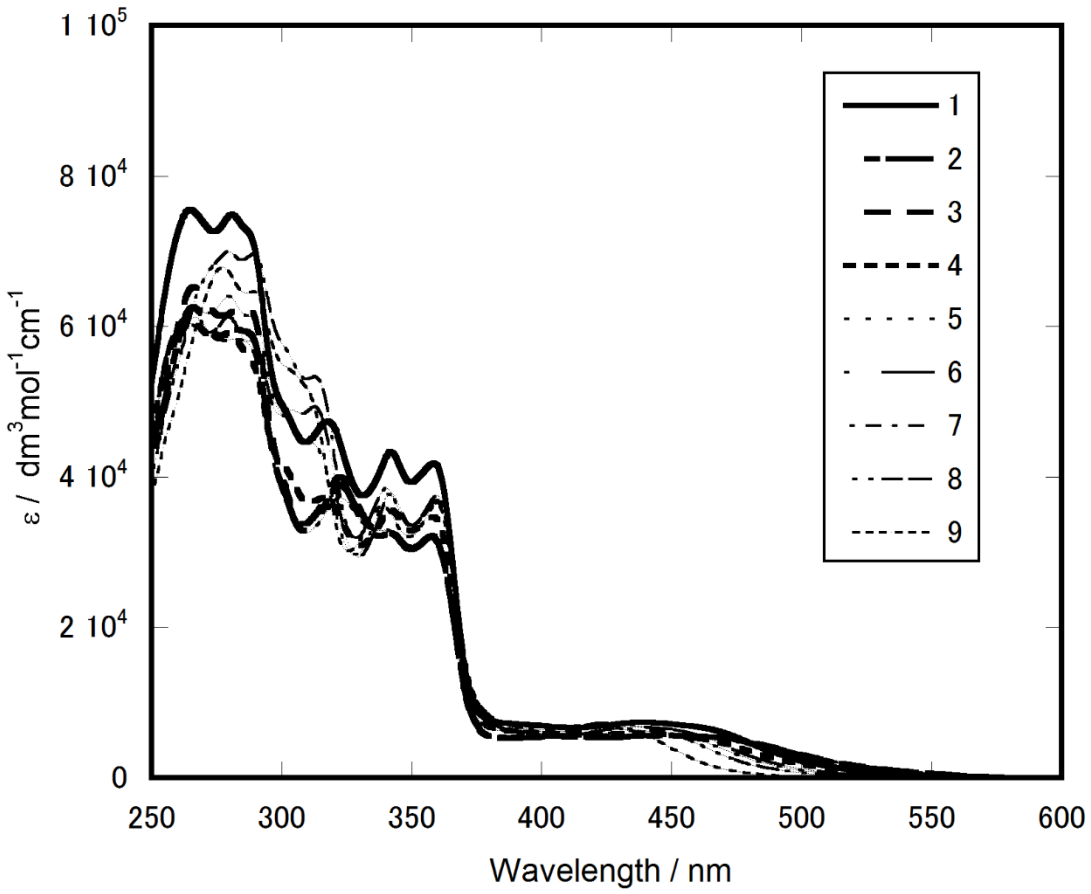

Fig. 1. UV-Vis absorption spectra of platinum organometallics **1-9** in CH_2Cl_2 at room temperature.

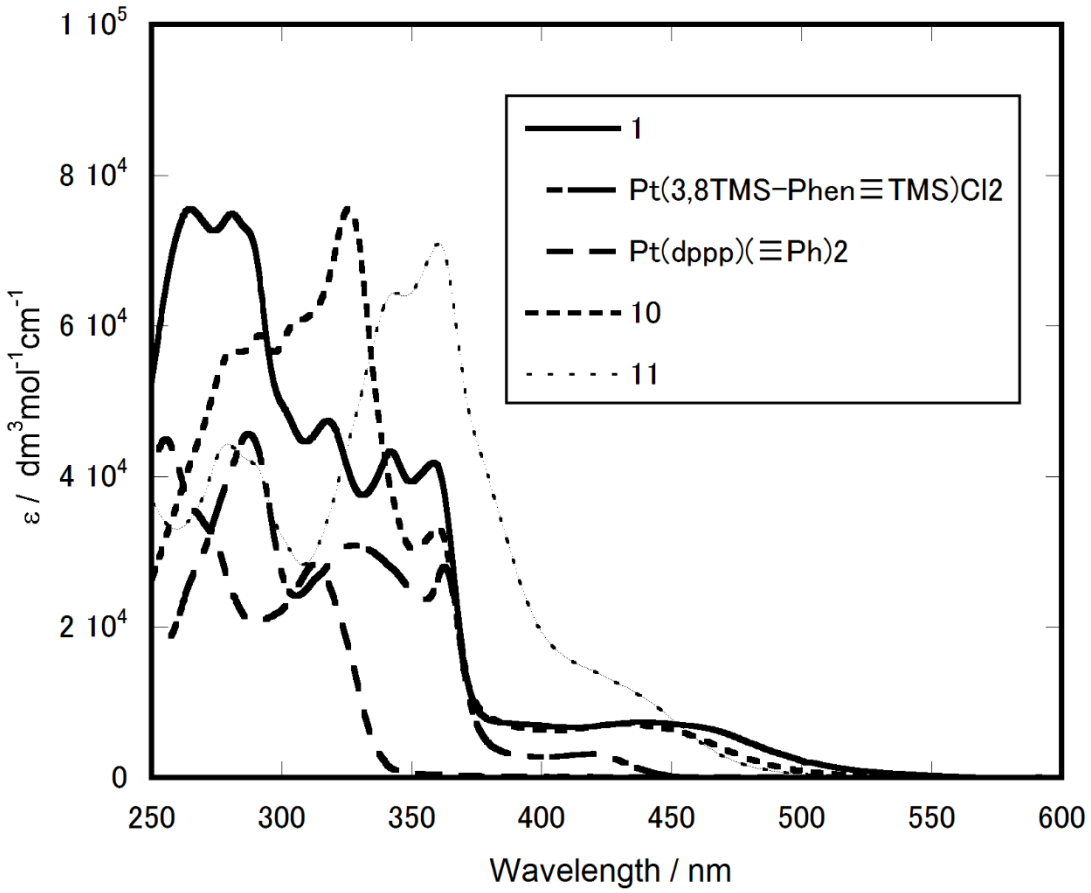

Fig. 2. UV-Vis absorption spectra of platinum organometallics **1**, **10**, **11**, Pt(3,8-Phen≡TMS)Cl_2, and Pt(dppp)(≡Ph)$_2$ in CH_2Cl_2 at room temperature.

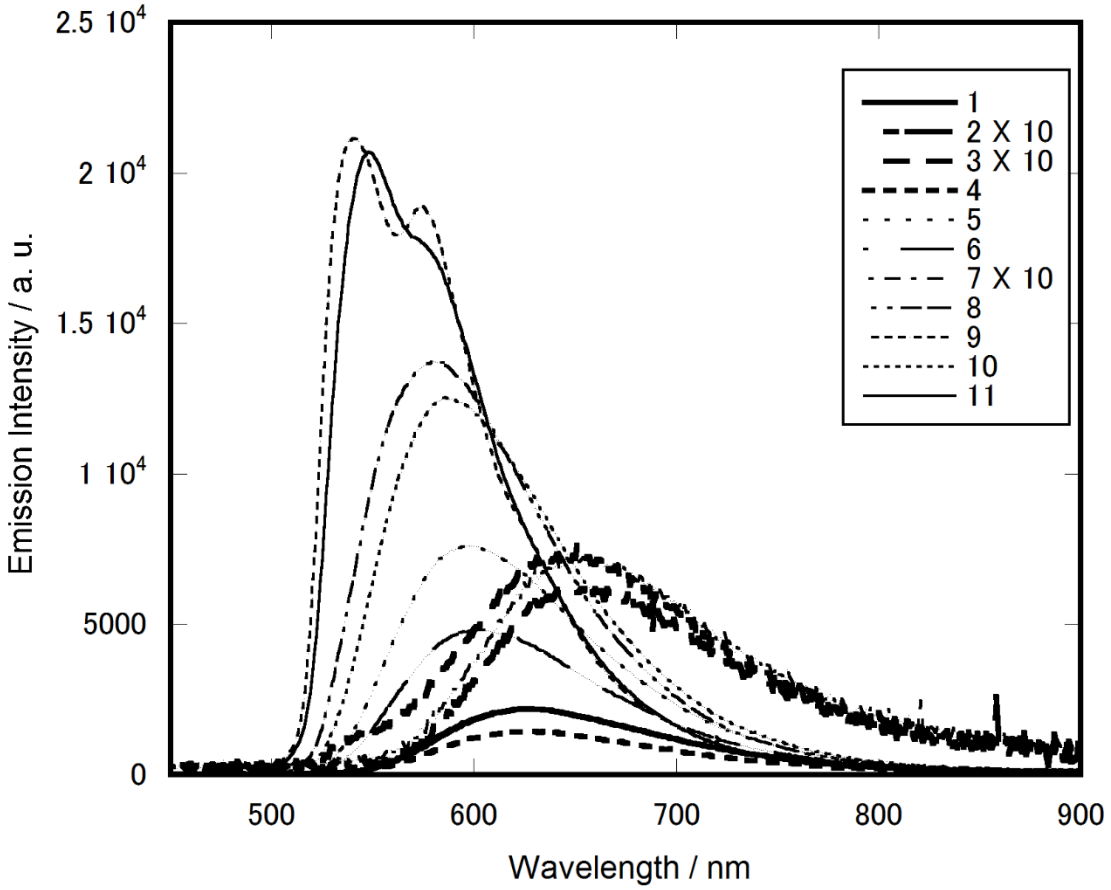

Fig. 3. Luminescence spectra of platinum organometallics **1-11** in CH_2Cl_2 at room temperature.

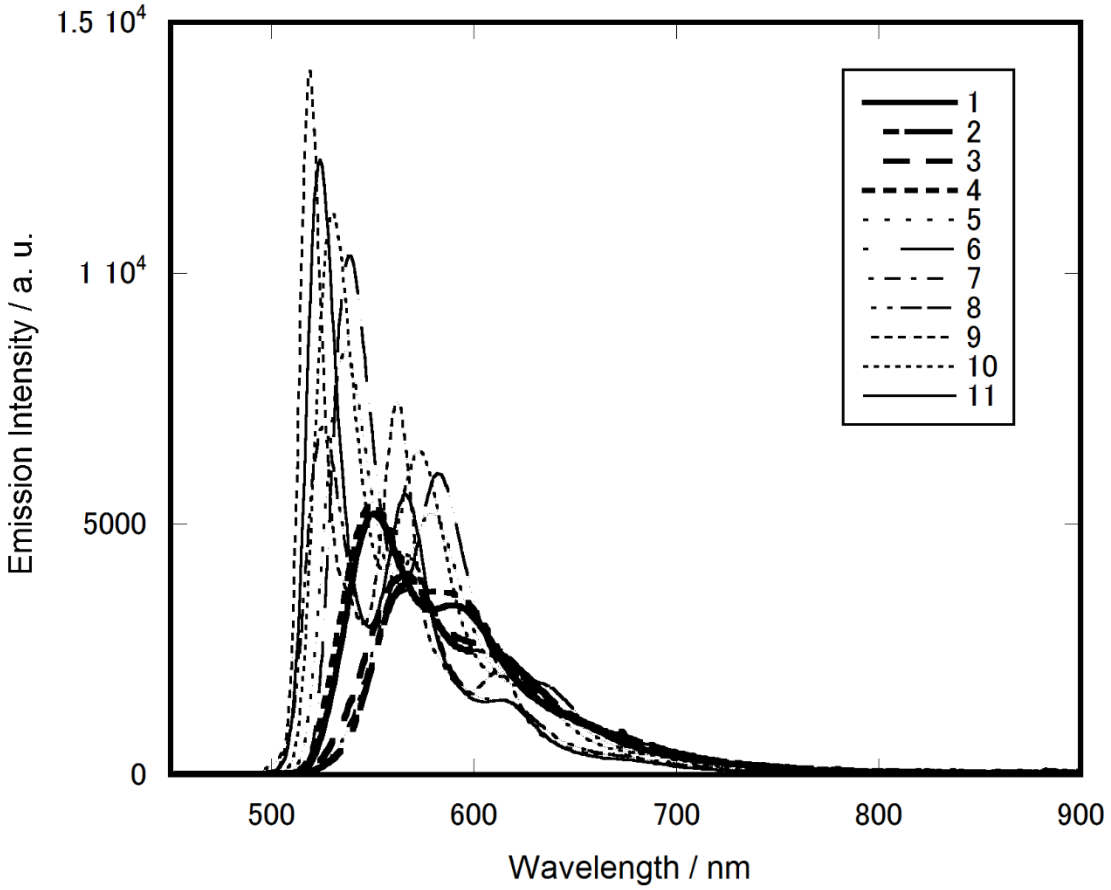

Fig. 4. Luminescence spectra of platinum organometallics **1-11** in 2-MeTHF at 77 k.

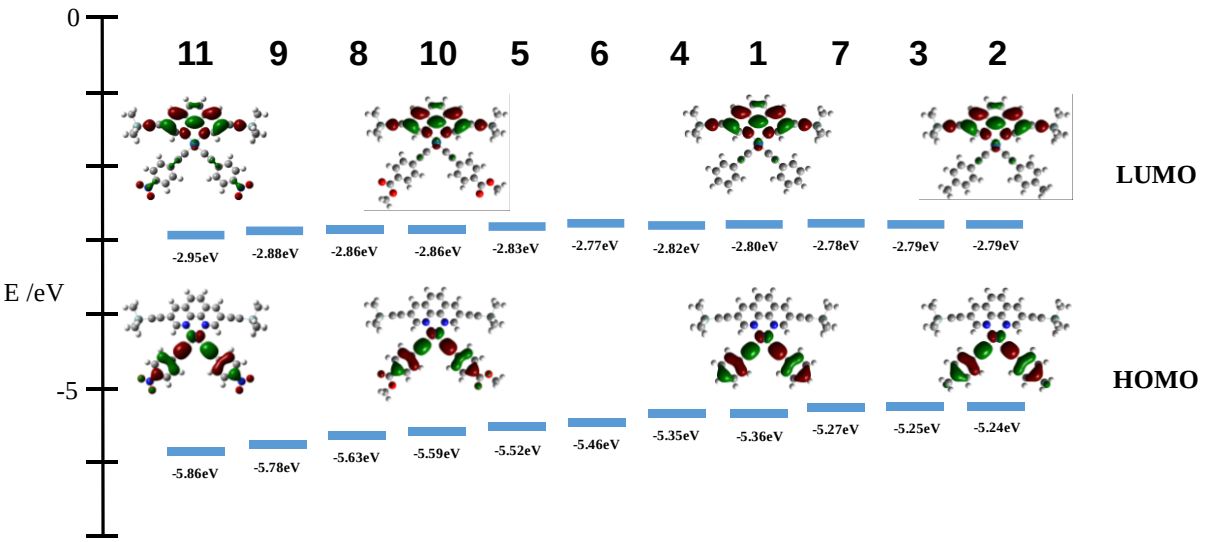

Fig. 5. Plots of the energy level of frontier molecular orbitals HOMO and LUMO for platinum organometallics **1** - **11** in a CH_2Cl_2 solution at room temperature under the singlet ground state by DFT calculation, together with the electron diagrams of the HOMO and LUMO for **1**, **2**, **10**, and **11** to demonstrate the similarity among their diagrams of all complexes.

Fig. 6

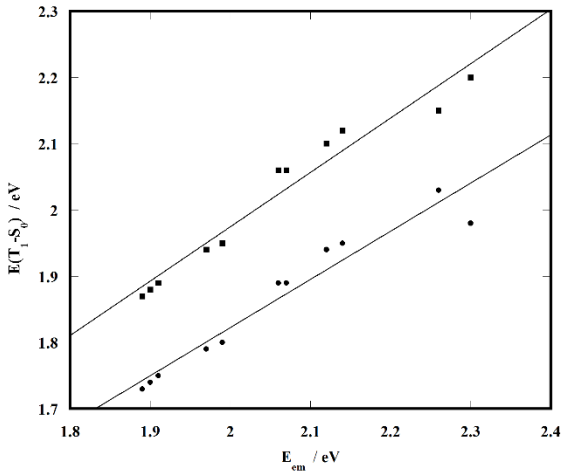

Fig. 6. Plots of the emission energy of the maximum intensity peak in the phosphorescent band, E_{em}, and the $E(T_1\text{-}S_0)_{DFT}$ from DFT (circle dot) or $E(T_1\text{-}S_0)_{TD\text{-}DFT}$ From TD-DFT (square dot) in terms of eV.

Graphical abstract